

A new poly(L-lactide)-grafted graphite oxide composite: Facile synthesis, electrical properties and crystallization behaviors

Lei Hua, Weihua Kai, JinJun Yang, Yoshio Inoue*

Department of Biomolecular Engineering, Tokyo Institute of Technology, Nagatsuta 4259-B55, Midori-ku, Yokohama 226-8501, Japan

ARTICLE INFO

Article history:

Received 9 June 2010

Received in revised form

18 July 2010

Accepted 26 July 2010

Available online 5 August 2010

Keywords:

Biodegradable polyester

Poly(L-lactide)

Graphite oxide

Electrical conductivity

Thermal degradation

Crystallization behaviors

ABSTRACT

A simple method was adopted to prepare poly(L-lactide)-grafted graphite oxide (PLLA-g-GO) by ring opening polymerization of L-lactide in the presence of graphite oxide (GO) with hydroxyl groups. GO was firstly treated with tolylene-2,4-diisocyanate (TDI) to create an anchor site on GO, and then reacted with 1,4-butanediol (BD) to afford functional hydroxyl groups grafted onto the surface of GO. So that, the dispersity of GO in the organic solution was enhanced. According to the thermogravimetric analysis (TGA), the organic composition of GO treated with TDI and BD (GO-TDI-OH) was estimated to be about 13 wt%. Also, using TGA, the composition of GO in the PLLA-g-GOs could be estimated. The hydroxyl groups on the GO surface acted as initiators for the ROP of L-lactide. Further, they also played a vital role in controlling the molecular weight of the PLLA. The synthesized PLLA-g-GOs were characterized by the FTIR, ¹HNMR and UV/Vis spectroscopies. The dispersion states of GO in the PLLA-g-GOs were investigated by wide angle x-ray diffraction patterns. According to differential scanning calorimeter study, it was found that GO platelets have nucleating effect on the crystallization of PLLA in the PLLA-g-GO. Additionally, the incorporation of GO improved the electrical conductivity of PLLA, indicating that GOs is a good conducting-modifiers for polymers.

© 2010 Elsevier Ltd. All rights reserved.

1. Introduction

Recently, biodegradable polymers are of increasing interest and attracting much attention from the material researchers and industry, owing to the increasing the environmental concerns about waste pollution [1,2]. Poly(L-lactide) (PLLA) is one of typical biodegradable polyesters and can be derived from natural starch-based resources. It has been manufactured on a commercial sale, and also used primarily for biomedical applications such as sutures and drug delivery systems [3–5]. PLLA is very promising material since it has good mechanical properties, thermal plasticity as compared with other biodegradable polymers [6]. Recently, the improvements of other physical properties of PLLA such as electrical properties and crystallization behaviors have aroused considerable interest. The electrical conducting biomaterials have been found to be widely studied in biomedical applications, such as tissue engineering. It has been reported that an electrical stimulus can enhance the outgrowth and spreading of neuritis of the cell, cell extension and cell growth [7]. For improvement of these properties,

the addition of various types of fillers is commercially advantageous, because the physical properties are readily manipulated by the type and concentration of fillers [8].

Natural flake graphite is composed of layered nanosheets [9]. Recently, graphite nanosheet-based polymer composites have been intensively studied because of their excellent electrical, thermal, and mechanical properties of graphite [10–15]. Natural graphite is anisotropic, being a good electrical and thermal conductor within layers, due to the in-plane metallic bonding, and a poor electrical and thermal conductor perpendicular to the layers, due to the weak van der Waals forces between the layers. The weak interplanar forces allow for certain atoms, molecules, and ions to intercalate into the interplanar spaces of the graphite [9]. The interplanar spacing is thus to be increased. However, unlike the layered clay, whose intercalation can be achieved by ionic exchange reactions, there are no reactive ionic groups on the surface of the layered graphite [11]. Thus, it is very difficult to prepare polymer intercalated or exfoliated polymer composite. Chen et al. [16] have successfully prepared carbon nanotube-PLLA nanocomposite using the surface-initiated ring opening polymerization (ROP) by the “grafting from” technique. The synthesis of PLLA comb polymer brushes on the surface of clay layers by in-situ ROP has been reported by Yang et al. [17] Paul et al. [18] had

* Corresponding author. Tel.: +81 45 924 5794; fax: +81 45 924 5827.

E-mail address: inoue.yaf@m.titech.ac.jp (Y. Inoue).

prepared exfoliated polylactide/clay nanocomposites by in-situ coordination-insertion polymerization and they also mentioned that the exfoliated structure of clay was more desirable than the intercalated one for the improved thermal stability of resulted exfoliated materials [16]. However, it is still a challenging work to obtain the complete exfoliated structure of clays in the polymer matrix although many methods, including in-situ polymerization, melt blending, and solution blending, have been developed [19–23]. Among these methods, the in-situ polymerization is a promising method for preparation of exfoliated nanocomposites [24]. In the intercalative polymerization technique, the monomer, together with the initiator and catalyst, is intercalated within the silicate or clay layers and the polymerization is initiated in-situ by either thermally or chemically. The chain growth on the surface of clay or silicate galleries triggers exfoliation of the clay or silicate composite [25].

Graphite oxide (GO) was proposed as the substitute of graphite for the fabrication of polymer/graphite composite [15,26–28]. The hydrophilic GO platelets prepared by oxidation of natural graphite is a lamellar solid with unoxidized aromatic regions and aliphatic regions containing large number of polar groups, such as hydroxyl, epoxide, and ether groups, as the result of oxidation [26,29,30]. Thus, the GO platelets are strongly hydrophilic and dispersible in water and alkaline solutions [29,31]. To enhance the dispersibility of GO in aprotic polar solvents and compatibility with polymer matrix, Stankovich et al. [32] have functionalized GO with isocyanates. Xu et al. [33] have treated the surface of GO with tolylene-2,4-diisocyanate (TDI) to create the anchor sites on GO and couple with amphiphilic oligoester through a “grafting to” approach to improve the dispersibility of modified GO in both water and organic media. The “grafting to” approach is to graft available polymers which normally possess terminal functional groups on the surface of substrate [34,35].

In our previous publication [14], we have studied ROP of ϵ -caprolactone using the OH groups as initiators on the surface of the GO platelets to prepare the poly(ϵ -caprolactone)-GO (PCL-GO) composite. Sn(Oct)₂ is known as an efficient catalyst for ROP of ϵ -caprolactone. The OH groups were proved to be highly efficient for initiating the polymerization and “grafting” the PCL chain onto the surface of the GO layers. The content of the surface OH functions was tunable as a parameter for controlling the molecular weight of PCL chain. Further, the PCL-GO composite showed exfoliation behavior, while the electrical properties of PCL-GO composite have not been investigated. In the present work, the PLLA-g-GO composite had been tried to prepare. However, the synthesis of PLLA-g-GO could not be achieved using the OH groups on the surface of GO as initiators, as the same method with that of PCL-GO. A more effective hydroxyl group initiator other than the hydroxyl group attached directly onto GO sheet as well as the enhanced dispersibility of graphite in organic media is needed.

In this paper, we report a facile method for preparation of PLLA-g-GO composites with improved electrical conductivity. Fully exfoliated PLLA-g-GO composites were synthesized by in-situ intercalative coordination-insertion polymerization of L-lactide directly from the interlayer organically modified GO. According to the method described by Xu et al. [33], GO was firstly treated with TDI to create the anchor sites on GO. Then, GO-TDI was reacted with 1,4-butanediol (BD) through the “grafting to” method to afford hydroxyl groups on the surface of GO. The BD-derived hydroxyl groups on the surface of GO will be effective as initiators for in-situ ROP of L-lactide. Further, the molecular weight of PLLA should be controllable by the hydroxyl groups on the TDI-DB of modified GO. The effects of GO on enhancement and improvement of crystallization behavior and electrical conductive properties of PLLA will be also studied.

2. Experimental

2.1. Materials

The graphite (Lot: M4P3193) and the potassium permanganate (Lot: M5E9617) were purchased from Nacalai Tesque, Inc. (Kyoto, Japan) and used as received. Sulfuric acid (>96%), nitric acid, hydrogen peroxide, Sn(Oct)₂, BD, acetone, anhydrous *N,N*-dimethylformamide (DMF), TDI and dehydrated toluene were purchased from Kanto Chemical Co. Inc. (Tokyo, Japan) and used also as received. The L-lactide was purchased from Sigma–Aldrich Co. (Tokyo, Japan) and recrystallized from ethyl acetate for 3 times before use. PLLA (Mn = 20,000) was synthesized by ROP of L-lactide and precipitated in ethanol for 3 times before use.

2.2. Preparation of GO

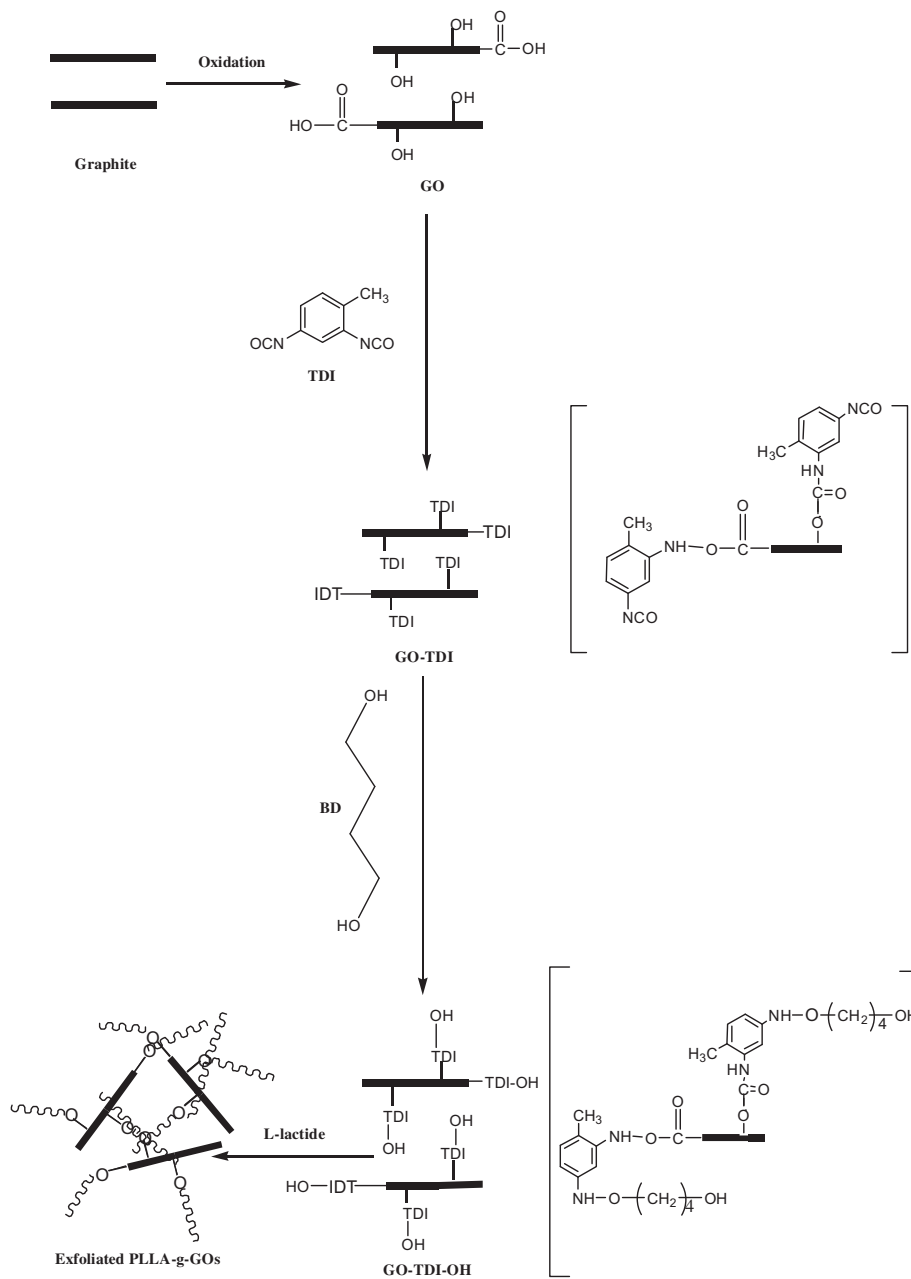
GO was prepared by modifying the method proposed by Hummers [29]. At first, graphite powder (5 g) was put into a 500-mL flask containing 68% nitric acid (33 mL) and sulfuric acid (>96%, 200 mL), stirred for 30 min on an ice-bath, and then potassium permanganate 30 g was added into the solution. The solution temperature was raised gradually to about 40 °C, maintained at this temperature for 30 min, and then the excess potassium permanganate was removed by the treatment with hydrogen peroxide and washed several times with distilled water. The product (GO) was obtained by centrifugation at 11,000 rpm for 20 min and dried in vacuum at 50 °C for 3 days. In order to hydrolyze the epoxy groups in GO, the parent GO was thermally treated in a vacuum oven at 100 °C for 24 h.

2.3. Preparation of isocyanate-treated GO (GO-TDI) and hydroxyl group grafted GO (GO-TDI-OH)

The procedure of the synthesis of GO-TDI-OH was shown in Scheme 1. GO-TDI-OH was prepared by modifying the method originally proposed by Xu et al. [33] The obtained GO was modified by an excess amount of TDI (GO: TDI = 1: 60 g/mmol). Subsequently, an excessive BD was added into this suspension. In this synthesis procedure, GO (2 g) was loaded into a 100 mL three-necked flask equipped with a magnetic stirring bar, and 100 mL DMF dehydrated was then added under nitrogen to create an in homogenous suspension. The TDI (2 g) was next added and the mixture was stirred under nitrogen at 80 °C for 24 h. After 24 h, the excessive BD (5 g) was added into the slurry reaction mixture under nitrogen atmosphere and then reacted for 24 h at 80 °C. The suspension was poured into acetone (50 mL) to coagulate the product, followed by centrifugation and washing several times to remove the unreacted BD. Finally, the resulting product (marked as GO-TDI-OH) was dried at 100 °C under vacuum for 48 h before use.

2.4. Synthesis of PLLA-g-GOs

At first, the ROP of L-lactide was proceed with OH groups on the surface of the unmodified GO as the initiators. However, the OH groups of GO is not so effective to initiate this polymerization. So, we tired to use the OH groups of the GO-TDI-OH to initiate ROP of L-lactide [36]. The synthetic route was shown in the Scheme 1 as described above. In the typical experiment, the desired amount of GO-TDI-OH (0.1 g or 0.3 g), monomer L-lactide (10 g) and dehydrated toluene (100 mL) were loaded into a dried three-necked flask equipped with a magnetic stirring bar. Then, the desired amount of catalysts Sn(Oct)₂, was added into the mixture. The three-necked flask was put into an oil bath at 110 °C under nitrogen atmosphere with vigorous stirring and then cooled to the room



Scheme 1. synthetic route of exfoliated PLLA-g-GOs.

temperature after reaction for 24 h. The obtained solid like black gel was diluted by chloroform (200 mL) and precipitated in hexane for three times, then washed with methanol to remove unreacted L-lactide. Finally the PLLA-g-GOs were dried in the vacuum oven at 40 °C before test. The code and composition of two samples were listed in Table 1.

2.5. Preparation of PLLA/GO-TDI-OH2.2 blend

In order to compare the nonisothermal crystallization behavior of PLLA-g-GO3 with PLLA/GO-TDI-OH2.2 blend, the PLLA/GO-TDI-OH2.2 blend, which has the same composition of GO as that of PLLA-g-GO3, was prepared. The desired amount of GO-TDI-OH powder and PLLA ($M_n = 20,000$) were mixed under stirring in 15 mL chloroform for 2 h at room temperature, and then the mixture was maintained at room temperature to afford the cast film.

2.6. Characterization

The Fourier transform infrared (FTIR) spectrum was observed at room temperature on a Perkin–Elmer Spectra 2000 single-beam IR spectrometer (Perkin–Elmer Japan Corp., Yokohama, Japan) with

Table 1

Sample code, weight composition of GO and the M_{narm} values of PLLA in the PLLA-g-GOs.

Samples code	GO-TDI-OH ^a (g)	L-lactide ^b (g)	GO ^c (wt %)	M_{narm} ^d (g/mol)
PLLA-g-GO 1	0.1	10	0.97	9250
PLLA-g-GO 3	0.3	10	2.2	6212

^a The weight of initiators GO-TDI-OH used in the ROP polymerization.

^b The weight of L-lactide monomer used in the ROP polymerization.

^c Weight composition of GO in the PLLA-g-GOs estimated from TGA analysis.

^d M_{narm} values of PLLA estimated from ¹HNMR.

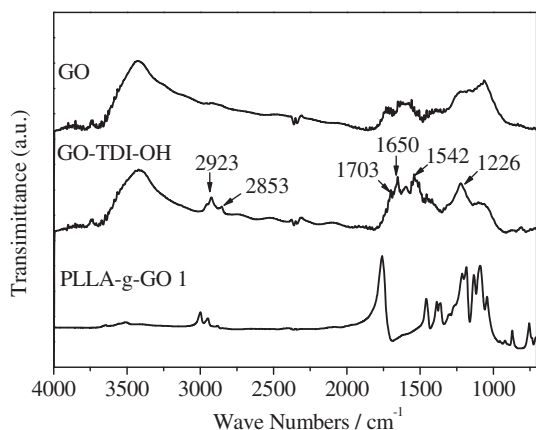


Fig. 1. FTIR spectra of GO, GO-TDI-OH and PLLA-g-GO1.

a resolution of 4 cm^{-1} . The specimens were dispersed into the KBr powder by mortar, and compressed to form disks.

The ultraviolet-visible (UV/Vis) spectra of the product were recorded on a JASCO V-550 UV/VIS spectrophotometer (JASCO, Tokyo, Japan) at room temperature.

Solution proton nuclear magnetic resonance (^1H NMR) spectra were recorded on a Bruker Ultrashield 600 MHz/54 mm NMR spectrometer at room temperature. CDCl_3 and tetramethylsilane (TMS) were used as solvent and chemical shift reference, respectively.

Thermogravimetric analysis (TGA) was carried out on a TG/DTA 220U (Seiko Instrument Co. Ltd, Tokyo Japan) with the Exstar 6000 Station. The samples (5–8 mg) were scanned from 20 to $550\text{ }^\circ\text{C}$ with the heating rate of $2\text{ }^\circ\text{C}/\text{min}$ and nitrogen gas purging.

The wide angle X-ray diffraction (WAXD) patterns of the sample films were recorded in the angle range of $5\text{--}40^\circ$ at scanning rate of $1\text{ }^\circ/\text{min}$ on a RU-200 X-ray diffractometer (Rigaku Co., Tokyo, Japan) at 40 kV and 200 mA at room temperature. Nickel-filtered $\text{Cu K}\alpha$ X-ray radiation ($\lambda = 0.15418\text{ nm}$) was used as source.

The process of nonisothermal crystallization was monitored by using a Pyris Diamond Differential scanning calorimeter (DSC) (Perkin–Elmer Japan Corp., Ltd. Yokohama, Japan) equipped with a Perkin–Elmer intracooler 2P cooling accessory. The temperature and the heat flow were calibrated using an indium standard with nitrogen gas purging. For the study of the melt nonisothermal crystallization, the specimen (5–8 mg) was firstly heated to $200\text{ }^\circ\text{C}$ in the DSC cell at a heating rate of $10\text{ }^\circ\text{C}/\text{min}$ and held at this temperature for 3 min, and then cooled to $0\text{ }^\circ\text{C}$ at a cooling rate of $10\text{ }^\circ\text{C}/\text{min}$.

The spherulite morphology was measured by polarized optical microscopy (POM) with an Olympus BX90 polarized microscope (Olympus Co. Tokyo, Japan) equipped with a Mettler FP82HT hot stage. The film samples were first heated from room temperature to $200\text{ }^\circ\text{C}$ and melted for 2 min. Subsequently, the samples were quenched to crystallize at $120\text{ }^\circ\text{C}$ at a cooling rate of $20\text{ }^\circ\text{C}/\text{min}$.

The electrical conductivity was measured by Mitusbishi Chemistry Hiresta-up MCP-HT450 with a URS probe (Seiko Instrument Co. Ltd., Tokyo, Japan). The hot pressed sample was cut into $4\text{ cm} \times 4\text{ cm}$ square specimens for testing. The applied voltage was set to 100 V. Volume resistivity (ρ_v) was measured by putting the probe on several points of the PLLA-g-GOs.

3. Results and discussion

According to the Scheme 1, it was found that graphite derivative was prepared firstly using a modifier TDI with bifunctional groups. The amide and carbamate esters were formed by treatment of GO with TDI, which lead to the derivatization of both the edge of carboxyl and surface hydroxyl functional groups. Then, the GO-TDI was modified by BD to afford the hydroxyl functional groups on the surface of GO through the “grafting to” method. Then, l -lactide was polymerized in bulk with various amounts of layered GO-TDI-OH. The polymerization was activated at about $110\text{ }^\circ\text{C}$ by $\text{Sn}(\text{Oct})_2$. The OH groups acted as an initiator in the dehydrated toluene solution and this polymerization process should proceed via an insertion–coordination mechanism [37]. That is, the polymerization proceeds through the insertion of the monomer into the “graphite-OH” bond of the initiator via the selective acyl-oxygen cleavage of the l -lactide. The details of the samples were shown in Table 1. As the OH groups of GO act as initiators for the polymerization, the molecular weight of the polymer chain grafted on the surface of graphite was controlled by the number of the hydroxyl groups. Based upon the method proposed by Xu et al. [33] by the treatment of GO with organic isocyanates, the increased number of the hydroxyl groups resulted in the decrease of the molecular weight of PLLA.

Fig. 1 shows the FTIR spectra of GO, GO-TDI-OH and PLLA-g-GO. GO shows the characteristic absorption peaks at 1732 and 1630 cm^{-1} , corresponding to the stretching mode of $\text{C}=\text{O}$ and $\text{C}-\text{OH}$, respectively. Upon treatment with TDI, the $\text{C}=\text{O}$ stretching vibration at 1732 cm^{-1} of GO becomes obscured by the appearance of a absorption peak at 1703 cm^{-1} that is attributable to the carbonyl stretching vibration of the carbamate esters of the GO-TDI-OH.

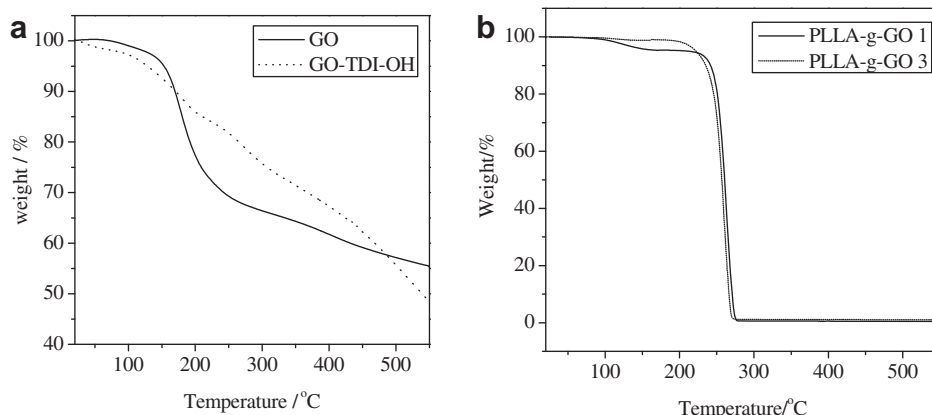


Fig. 2. Thermal degradation curves of (a) GO and GO-TDI-OH and (b) PLLA-g-GO1 and PLLA-g-GO3. Scanning rate $2\text{ }^\circ\text{C}/\text{min}$.

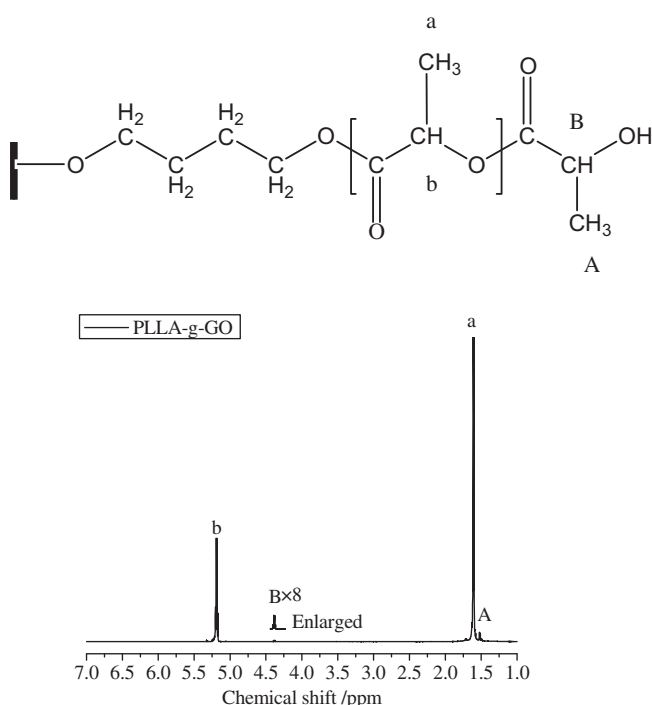


Fig. 3. 600 MHz ^1H NMR spectrum of the PLLA-g-GO sample.

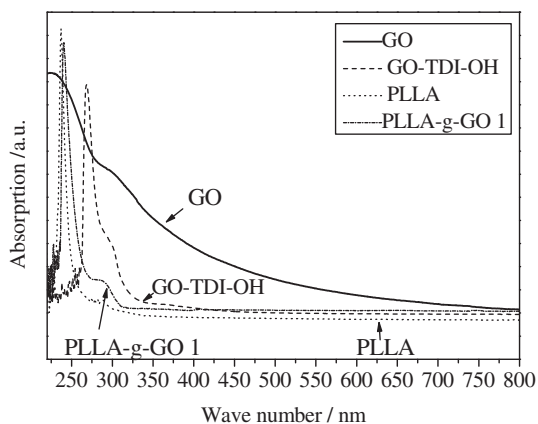


Fig. 4. UV/Vis spectra of PLLA-g-GO1, PLLA, GO and GO-TDI-OH.

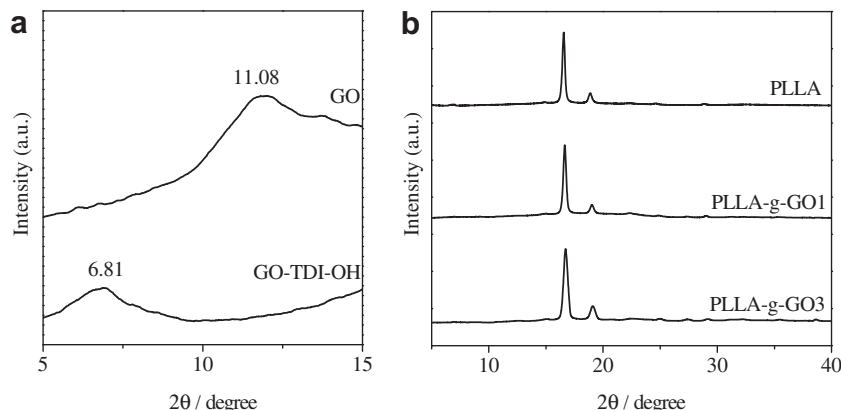


Fig. 5. Wide angle x-ray diffraction patterns of (a) GO, GO-TDI-OH, and (b) PLLA, PLLA-g-GO1 and PLLA-g-GO3.

A band at 1650 cm^{-1} could be assigned to the amide carbonyl stretching mode. The band at 1542 cm^{-1} is originated from either amides or carbamates esters and corresponds to the coupling of the C–N stretching vibration with the CHN deformation vibration [32]. Strong absorption bands, which are due to the $-\text{CH}_2-$ stretching vibration, appear at 2923 and 2853 cm^{-1} after reaction with BD. The 1226 cm^{-1} band is corresponding to the C–OH stretching vibration. On the other hand, the FTIR spectrum of the GO in the PLLA-g-GO is masked by the peaks of PLLA due to the relatively less content of GO.

In order to analyze the organic modification of GO-TDI-OH, GO and GO-TDI-OH were subjected to thermal degradation analysis in N_2 . Fig. 2(a) shows the TGA thermal degradation curves of GO and GO-TDI-OH. GO starts to lose their weight mass upon heating at the temperature region below 100°C . The small weight loss found for GO at the temperature range from 100 to 150°C is due to the evaporation of physically absorbed water. The weight loss of GO at the temperature range from 150 to 250°C is attributed to pyrolysis of the liable oxygen-containing functional groups, yielding CO, CO_2 and water vapor. At the temperature above 250°C , the weight loss of GO would also be due to release of oxygen away from GO leaving residual carbon [27,38].

On the other hand, the small weight loss found for GO-TDI-OH in the temperature range from 100 to 150°C is due to the evaporation of absorbed water. Further, the weight loss of GO-TDI-OH decrease from 200 to 450°C , which is due to the pyrolysis of the liable oxygen-containing functional groups and the decomposition of the organic diisocyanates in the GO-TDI-OH with gradually ascending the temperature [39]. Moreover, when the temperature is above 450°C , the weight decrease of GO-TDI-OH would be due to the elimination of BD chain and the loss of oxygen from the GO skeleton. When the temperature reaches to 550°C , the GO-TDI-OH also leaves residual carbon, which is the same element with residual part of the GO [40]. Furthermore, the residual mass fraction of GO and GO-TDI-OH is 55 and $48\text{ wt}\%$ respectively. The residual mass of GO is $55\text{ wt}\%$, so the degraded part of GO is $45\text{ wt}\%$. Here, the GO-TDI-OH could be considered as two parts: GO and the modification. Based on weight ratio of residual mass and degradation part of GO, the degraded part of GO in GO-TDI-OH could be estimated to be about $39\text{ wt}\%$, the total composition of GO in GO-TDI-OH is about $87\text{ wt}\%$. It is easy to estimate the modification of GO-TDI-OH is about $13\text{ wt}\%$.

In order to determine the weight composition of GO grafted onto the PLLA matrix in the PLLA-g-GOs, the TGA measurement was also performed. Fig. 2(b) is the thermal degradation curves of PLLA-

g-GO1 and PLLA-g-GO3. The major and sharp weight loss of PLLA-g-GOs occurring at the temperature range from 210 to 270 °C is due to the decomposition of the PLLA matrix. When the temperature reached to the 550 °C, the residual mass of PLLA-g-GO1 and PLLA-g-GO3 is about 0.47 and 1.07 wt% respectively. However, it is found that the residual part of GO-TDI-OH around 550 °C is about 48 wt% in the Fig. 2(a). According to the thermal analysis of Fig. 2(a) and (b), it is easy to estimate the weight composition of GO in the PLLA-g-GO1 and PLLA-g-GO3 is about 0.97 and 2.2 wt%, respectively. The data were summarized in Table 1. The weight composition of GO in the PLLA-g-GO1 and PLLA-g-GO3 is litter lower than the theoretical value, 1 and 3 wt%, respectively.

Fig. 3 shows the 600 MHz ¹H NMR spectrum of the PLLA-g-GO sample. It shows the typical resonances for PLLA, indicating the

production of PLLA. The peak appeared at 1.55 ppm is assigned to the -CH₃ groups of PLLA. The peak b at 5.16 ppm is methine protons -CH-, while B at 4.36 ppm is corresponding to the methine group -CH- located at the end of the chain which is adjacent to the terminal hydroxyl groups.¹⁷ According to the ¹H NMR spectrum, using the relative intensities of two peaks B and b, the number average molecular weight of every PLLA arm chain (M_{narm}) on the surface of GO was calculated as shown in Table 1. It is obvious that with increasing the GO-TDI-OH content the M_{narm} of PLLA decreased. This is due to the increased ratio of initiator to monomer. Here, GPC was not used to estimate the M_{narm} of PLLA grafting on the surface of GO. Because the PLLA chain is attached on the surface of GO, the size of which is much larger than that of pores of gels packed in the column of GPC.

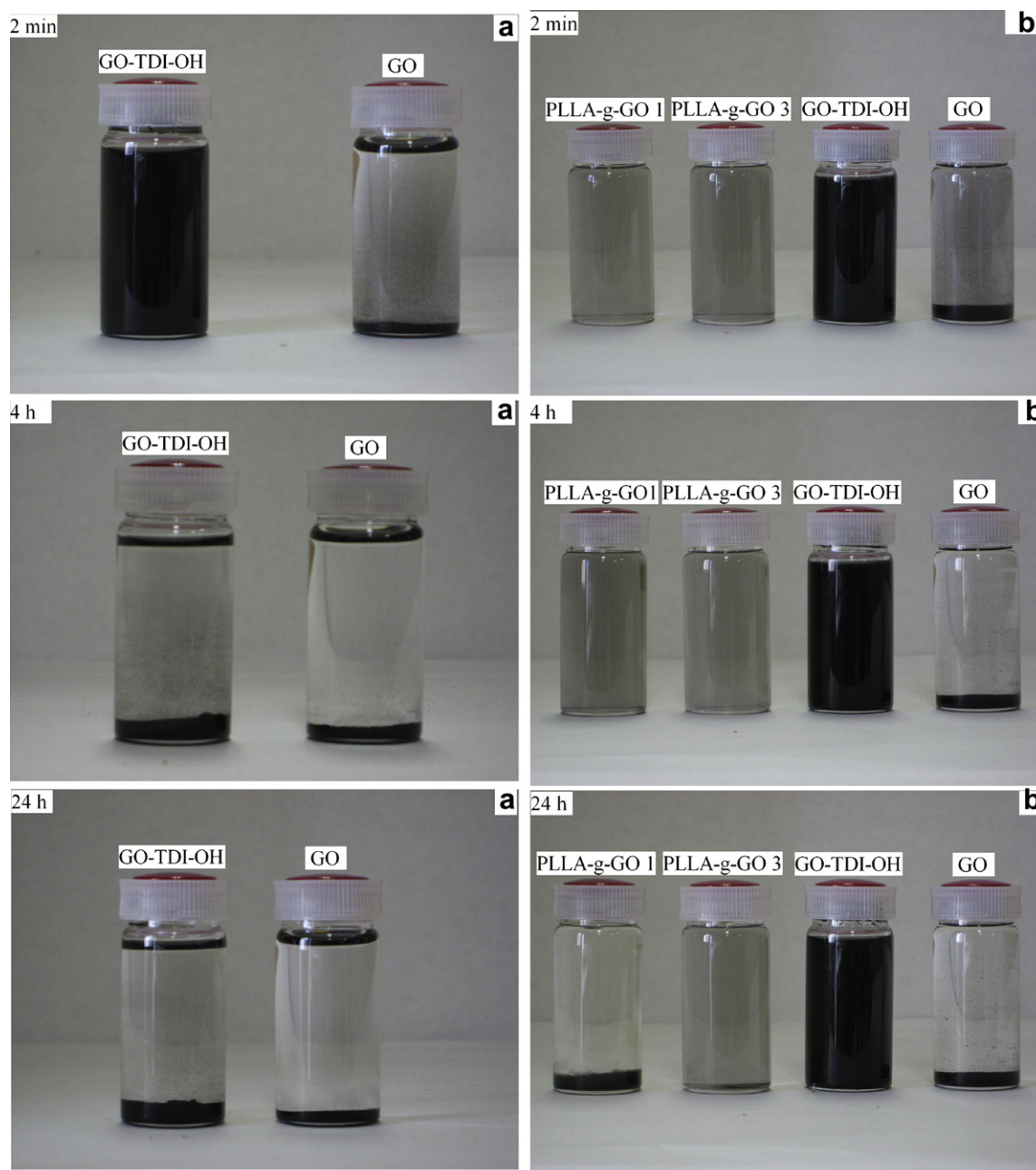


Fig. 6. (a) Dispersivity of GO, GO-TDI-OH in the toluene dehydrated, and (b) GO, GO-TDI-OH PLLA-g-GO1 PLLA-g-GO3 in the chloroform. After 2 min, 4 h, 24 h at 0.01 g/mL concentration.

Fig. 4 are shown the UV/Vis spectra of PLLA-g-GO composite, PLLA, GO and GO-TDI-OH. The UV/Vis spectrum of GO was observed in the aqueous solution, while those of GO-TDI-OH, PLLA, and PLLA-g-GO1 were in the DMF solution. GO shows very broad absorption with continuously decreasing intensity ranged from 220 to 800 nm. On the other hand, GO-TDI-OH shows the absorption in the range from 250 to 330 nm and no absorption peak is observed in the 330 to 800 nm range. Further, PLLA shows characteristic peaks in the wave length region shorter than 250 nm, while no evident absorption in the higher wave length region. In the absorption spectrum in the range from 220 to 320 nm, the PLLA-g-GO1 shows absorption with special features characteristics for both PLLA and GO-TDI-OH, indirectly indicating that the PLLA chain was grafted onto the surface of GO.

Fig. 5 shows the WAXD patterns of GO, GO-TDI-OH, PLLA, PLLA-g-GO1 and PLLA-g-GO3 samples. The PLLA, PLLA-g-GO1 and PLLA-g-GO3 samples were prepared by melt press at 200 °C and crystallized at 90 °C for 2–3 h in vacuum oven. According to Fig. 5 (a), the diffraction peak of pristine GO is observed at about $2\theta = 11.08^\circ$, corresponding to the interlayer spacing of 0.79 nm, while that of the GO-TDI-OH platelets shifts to low $2\theta = 6.81^\circ$ and thus the interlayer spacing is increased to 1.3 nm due to presence of the TDI and BD between the sheets of the GO [39]. As the interlayer spacing of the natural graphite is only about 0.33 nm [41,42], Upon oxidation and modification, the interlayer spacing of the graphite increased significantly from 0.33 to 1.3 nm.

Meanwhile, the WAXD patterns of PLLA-g-GOs are shown in Fig. 5(b). The PLLA-g-GOs show a typical WAXD pattern of PLLA, while there are no peaks of layered structure of GO-TDI-OH in the PLLA-g-GO composites indicating that the layer structured GO-TDI-OH lost its ordered structure. The lack of the diffraction peaks of GO-TDI-OH could be attributed to the complete exfoliation and random distribution of the GO-TDI-OH platelets within the PLLA matrix. So, an exfoliated structure of graphite is obtained for the PLLA-g-GO composites.

Fig. 6 shows the photographs of the dispersity of GO, GO-TDI-OH dispersed in dehydrated toluene, and those of GO, GO-TDI-OH, PLLA-g-GO1 and PLLA-g-GO3 in chloroform with 0.01 g/mL concentration after the preparation of 2 min, 4 h and 24 h. Remarkably, when the GO particles were added to the chloroform, the particles at first suspended in the solution, while they almost completely precipitated after 4 h and kept this precipitated state for 24 h, while the GO-TDI-OH particles were found to disperse in toluene and chloroform for a long time. In other words, the dispersity of GO-TDI-OH is better than GO in the dehydrated toluene and chloroform media. The dispersity of GO is increased in the toluene solvent by treatment with TDI and BD, which provided a possible way to initiate the polymerization of ϵ -lactide in the toluene solvent. Meanwhile, PLLA-g-GO1 also shows the good solubility in the chloroform due to the presence of the PLLA chain on the surface of the GO platelets.

The melt crystallization behavior was investigated by DSC measurements, Fig. 7(a) shows DSC cooling scan thermogram of PLLA (Mn = 20,000), PLLA-g-GO1, PLLA-g-GO3 and PLLA/GO-TDI-OH2.2 blend at the cooling rate of 10 °C/min. A neat PLLA crystallizes in a broad crystallization temperature range with the peak crystallization appearing at 101.1 °C. The crystallization peak temperature of PLLA in PLLA-g-GO1 occurs at 101.2 °C and the temperature range of crystallization is broad, while the crystallization temperature of the PLLA-g-GO3 shifts to the higher temperature at 109.6 °C and the temperature range becomes narrow.

The nonisothermal crystallization behavior of PLLA/GO-TDI-OH2.2 blend, which has the same composition of GO as that of PLLA-g-GO3, was performed to compare with PLLA-g-GO3. The

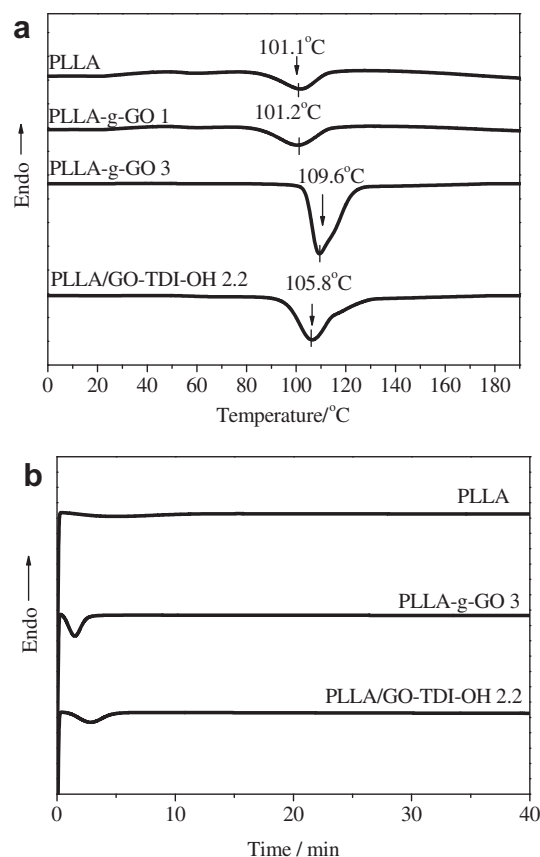


Fig. 7. (a) DSC cooling scan thermogram of PLLA (Mn = 20,000), PLLA-g-GO1, PLLA-g-GO3 and PLLA/GO-TDI-OH2.2 blend at the cooling rate of 10 °C/min. (b) the isothermal crystallization behavior of PLLA, PLLA-g-GO3 and PLLA/GO-TDI-OH2.2 at 120 °C.

crystallization temperature of PLLA in the PLLA/GO-TDI-OH2.2 is about 105.8 °C. As compared with neat PLLA, the crystallization temperature of PLLA in the PLLA-g-GO1 has not been increased. However, the crystallization temperature of PLLA in the PLLA-g-GO3 was increased to 109.6 °C. Further, the crystallization temperature of PLLA in the PLLA/GO-TDI-OH2.2 also shows a little increase as compared with neat PLLA, suggesting that the GO platelets incorporated into the PLLA matrix has nucleating effect on the crystallization of PLLA in the PLLA-g-GO3. Based on the comparison between the results of PLLA-g-GO3 and PLLA/GO-TDI-OH2.2 blend, a nucleating effect found in the melt crystallization of PLLA-g-GO3 is not only due to the individual GO platelets into the PLLA matrix, but also due to the tight bonding between the GO platelets. The GO platelets in the PLLA-g-GO1 shows little the nucleating effect on the crystallization of PLLA regardless of the tight bonding between the GO platelets and PLLA chains due to the lower amount of GO in the PLLA-g-GO1 (0.97 wt %, see Table 1).

The nucleating effect of the exfoliated GO platelets on the crystallization of PLLA in the PLLA-g-GO3 is also confirmed by comparing the isothermal crystallization behavior of PLLA, PLLA-g-GO3 and PLLA/GO-TDI-OH2.2 blend at 120 °C as shown in Fig. 7(b). Clearly, the isothermal crystallization rate of PLLA-g-GO3 is much higher than that of pure PLLA, while is a little higher than that of PLLA/GO-TDI-OH 2.2, which can be explained by the reduced mobility of PLLA chain when “grafting to” the graphite surface, leading to a better interaction between PLLA and GO sheets and lower mobility of PLLA segment.

The nucleating effect of the exfoliated GO platelets on the crystallization of PLLA was also confirmed by POM. Fig. 8 shows the POM photographs of pure PLLA and PLLA-g-GO3 samples crystallized at $T_c = 120^\circ\text{C}$. The spherulites of PLLA-g-GO3 are smaller in size and larger in numbers than those of the pure PLLA. These results are indicative of the increased nucleation density in the PLLA-g-GO3. This might be explained by a heterogeneous nucleation initiated by the introduction of GO into PLLA [43]. Grafted PLLA chain bonding to the surface of graphite layer increases the interaction between PLLA chain and graphite platelets. These GO platelets, to which the PLLA chains grafted, might act as the nucleating agent to initiate nucleation and increase the nucleation density for PLLA crystallization.

Fig. 9 shows the relationship between the volume electrical conductivity and the PLLA-g-GOs with different GO content. Although the graphite is anisotropic, being a good electrical and thermal conductor within layers, electrical conductivity of GO was decreased greatly after oxidation for conjugated structure of GO, however, there still have some conjugated structure that resulted in the conductivity of GO. When the volume voltage was set to 100 V, the electrical conductivity of PLLA was negligible resembling that of an insulator. The electrical conductivity of PLLA was considered as 0 in Fig. 9. With increasing the weight content of the GO platelets in the composites from 1 to 3 wt %, the electrical conductivity of composites was increased. Like most polymers, PLLA is not electrically conductive at the room temperature, the addition of GO improved the electrical conductivity of PLLA-g-GOs was shown to be good conducting filler for the polymers.

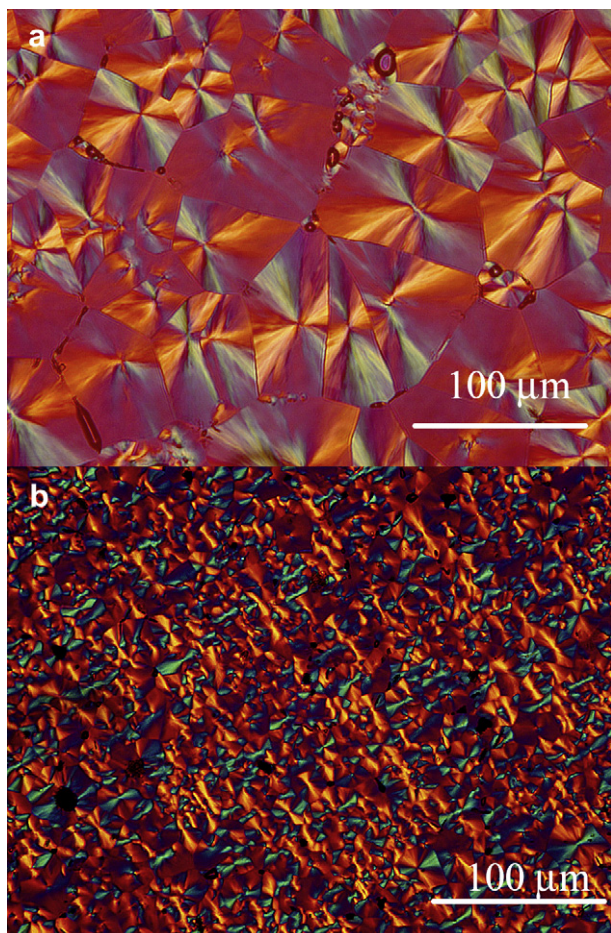


Fig. 8. The POM photos of (a) pure PLLA ($M_n = 20,000$), and (b) PLLA-g-GO3 crystallized at $T_c = 120^\circ\text{C}$.

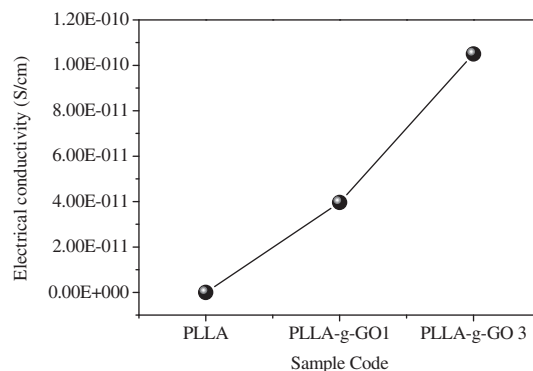


Fig. 9. The relationship between the volume electrical conductivity and the PLLA-g-GOs with different GO content.

4. Conclusion

An exfoliated PLLA-g-GO composite was successfully prepared by in-situ coordinative polymerization of L-lactide by ROP. The dispersibility of GO in the organic media was improved after modification of BD. And the modified GO afforded active hydroxyl groups on the surface of GO, which provided a possible way to initiate the L-lactide in the toluene dehydrated solution. The formation of PLLA-g-GOs was confirmed by FTIR, ^1H NMR and UV/Vis spectra. The hydroxyl functions composition played a vital role in controlling the molecule weight of the PLLA. A nucleating effect of GO on the crystallization of PLLA was found in the melt crystallization of PLLA-g-GO3 as compared with PLLA/GO-TDI-OH2.2. The first reason was explained as the disordered GO platelets dispersed randomly in the PLLA matrix, the other reason was due to the PLLA chain grafting on the surface of GO which increased the interaction between PLLA chain and GO. Further, the electrical conductivity of the PLLA-g-GOs was increased in the presence of graphite.

In conclusion, this facile method provides an effective way to prepare biodegradable polymer grafted inorganic filler, which wide applications for the biodegradable polymer in the future.

References

- [1] Inoue Y, Yoshie N. Structure and physical properties of bacterially synthesized polyesters. *Prog Polym Sci* 1992;17(4):571–610.
- [2] Okada M. Chemical synthesis of biodegradable polymers. *Prog Polym Sci* 2002;27(1):87–113.
- [3] Fukushima K, Chang YH, Kimura Y. Enhanced stereocomplex formation of poly(L-lactic acid) and poly(D-lactic acid) in the presence of stereoblock poly(lactic acid). *Macromol Biosci* 2007;7(6):829–35.
- [4] Xu H, Teng C, Yu M. Improvements of thermal property and crystallization behavior of PLLA based multiblock copolymer by forming stereocomplex with PDLA oligomer. *Polymer* 2006;47(11):3922–8.
- [5] Drumright RE, Gruber PR, Henton DE. Polylactic acid technology. *Adv Mater* 2000;12(23):1841–6.
- [6] Bordes P, Pollet E, Avérous L. Nano-biocomposites: biodegradable polyester/nanoclay systems. *Prog Polym Sci* 2009;34(2):125–55.
- [7] Hong L, Zhang X, Hu J, Lang L, Zhang P, Wang Y, et al. Synthesis of biodegradable and electroactive multiblock polylactide and aniline pentamer copolymer for tissue engineering applications. *Biomacromolecules* 2008;9(3):850–8.
- [8] Tsuji H, Kawashima Y, Takikawa H, Tanaka S. Poly(L-lactide)/nano-structured carbon composites: conductivity, thermal properties, crystallization, and biodegradation. *Polymer* 2007;48(14):4213–25.
- [9] Chung DDL. Graphite. *J Mater Sci* 2002;37(8):1475–89.
- [10] Zhang M, Li D, Wu D, Yan C, Lu P, Qiu G. Poly(ethylene terephthalate)/expanded graphite conductive composites: structure, properties, and transport behavior. *J Appl Polym Sci* 2008;108(3):1482–9.
- [11] Zheng W, Wong S, Sue H. Transport behavior of PMMA/expanded graphite nanocomposites. *Polymer* 2002;43(25):6767–73.

- [12] Pan Y, Yu Z, Ou Y, Hu G. A new process of fabricating electrically conducting nylon 6/graphite nanocomposites via intercalation polymerization. *J Polym Sci Part B: Polym Phys* 2000;38(12):1626–33.
- [13] Gopakumar T, Pagé D. Polypropylene/graphite nanocomposites by thermokinetic mixing. *Polym Eng Sci* 2004;44(6):1162–9.
- [14] Hua L, Kai W, Inoue Y. Synthesis and characterization of poly(ϵ -caprolactone)-graphite oxide composites. *J Appl Polym Sci* 2007;106(3):1880–4.
- [15] Kai WH, Hirota Y, Hua L, Inoue Y. Thermal and mechanical properties of a poly(ϵ -caprolactone)/graphite oxide composite. *J Appl Polym Sci* 2007;107(3):1395–400.
- [16] Chen GX, Kim HS, Shim JH, Yoon JS. Role of epoxy groups on clay surface in the improvement of morphology of poly(l-lactide)/clay composites. *Macromolecules* 2005;38(9):3738–44.
- [17] Yang Y, Wu D, Li C, Liu L, Cheng X, Zhao H. Poly(l-lactide) comb polymer brushes on the surface of clay layers. *Polymer* 2006;47(21):7374–81.
- [18] Paul MA, Alexandre M, Degée P, Calberg C, Jérôme R, Dubois P. Exfoliated polylactide/clay nanocomposites by in-situ coordination-insertion polymerization. *Macromol Rapid Commun* 2003;24(9):561–6.
- [19] Cui L, Tarrte NH, Woo SI. Effects of modified clay on the morphology and properties of PMMA/clay nanocomposites synthesized by in situ polymerization. *Macromolecules* 2008;41(12):4268–74.
- [20] Meneghetti P, Qutubuddin S. Synthesis of poly(methyl methacrylate) nanocomposites via emulsion polymerization using a Zwitterionic surfactant. *Langmuir* 2004;20(8):3424–30.
- [21] Zhao Q, Samulki ET. In situ polymerization of poly(methyl methacrylate)/clay nanocomposites in supercritical carbon dioxide. *Macromolecules* 2005;38(19):7967–71.
- [22] Shah RK, Paul DR. Organoclay degradation in melt processed polyethylene nanocomposites. *Polymer* 2006;47(11):4075–84.
- [23] Huang YJ, Yang KF, Dong JY. Copolymerization of ethylene and 10-undecen-1-ol using a montmorillonite-intercalated metallocene catalyst: synthesis of polyethylene/montmorillonite nanocomposites with enhanced structural stability. *Macromol Rapid Commun* 2006;27(15):1278–83.
- [24] Zanetti M, Lomakin A, Camino G. Polymer layered silicate nanocomposites. *Macromol Mater Eng* 2000;279(1):1–9.
- [25] Tasdelen MA, Camp WV, Gorthals E, Dubois P, Prez FD, Yagci Y. Poly-tetrahydrofuran/clay nanocomposites by in situ polymerization and “click” chemistry processes. *Macromolecules* 2008;41(16):6035–40.
- [26] Han Y, Lu Y. Preparation and characterization of graphite oxide/polypyrrole composites. *Carbon* 2007;45(12):2394–9.
- [27] Matsuo Y, Miyabe T, Fukutsuka T, Sugie Y. Preparation and characterization of alkylamine-intercalated graphite oxides. *Carbon* 2007;45(5):1005–12.
- [28] Wang G, Yang Z, Li X, Li C. Synthesis of poly(aniline-co-o-anisidine)-intercalated graphite oxide composite by delamination/reassembling method. *Carbon* 2005;43(12):2564–70.
- [29] Lerf A, He H, Forster M, Klinowski J. Structure of graphite oxide revisited. *J Phys Chem B* 1998;102(23):4477–82.
- [30] Kovtyukhova N, Olliver P, Martin B, Mallouk T, Chizhik S, Buzaneva E. Layer-by-layer assembly of ultrathin composite films from micron-sized graphite oxide sheets and polycations. *Chem Mater* 1999;11(3):771–8.
- [31] Liu P, Gong K, Xiao P, Xiao M. Preparation and characterization of poly(vinyl acetate)-intercalated graphite oxide nanocomposite. *J Mater Chem* 2000;36(10):933–5.
- [32] Stankovich S, Piner RD, Nguyen ST, Ruoff RS. Synthesis and exfoliation of isocyanate-treated graphene oxide nanoplatelets. *Carbon* 2006;44(15):3342–7.
- [33] Xu C, Wu X, Zhu J, Wang X. Synthesis of amphiphilic graphite oxide. *Carbon* 2008;46(2):386–9.
- [34] Ranjan R, Brittain W. Combination of living radical polymerization and click chemistry for surface modification. *Macromolecules* 2007;40(18):6217–23.
- [35] Liu Y, Chen W. Modification of multiwall carbon nanotubes with initiators and macroinitiators of atom transfer radical polymerization. *Macromolecules* 2007;40(25):8881–6.
- [36] Wang JL, Dong CM. Synthesis, sequential crystallization and morphological evolution of well-defined star-shaped poly(ϵ -caprolactone)-b-poly(L-lactide) block copolymer. *Macromol Chem Phys* 2006;207(5):554–62.
- [37] Duda A, Penczek S, Kowalski A, Libiszowski J. Polymerizations of ϵ -caprolactone and L, L-dilactide initiated with stannous octoate and stannous butoxide- a comparison. *Macromol Symp* 2000;153(1):41–53.
- [38] Stankovich S, Dikin DA, Piner RD, Kohlhaas KA, Kleinhammes A, Jia Y, et al. Synthesis of graphene-based nanosheets via chemical reduction of exfoliated graphite oxide. *Carbon* 2007;45(7):1558–65.
- [39] Zhang DD, Zu SZ, Han BH. Inorganic-organic hybrid porous materials based on graphite oxide sheets. *Carbon* 2009;47(13):2993–3000.
- [40] Matsuo Y, Tabata T, Fukunaga T, Fukutsuka Y, Sugie Y. Preparation and characterization of silylated graphite oxide. *Carbon* 2005;43(14):2875–82.
- [41] Zheng GH, Wu JS, Wang WP, Pan CY. Characterizations of expanded graphite/polymer composites prepared by in situ polymerization. *Carbon* 2004;42(14):2839–47.
- [42] Kotov NA, Dekany I, Fendler JH. Micelles, monolayers and biomembranes. *Adv Mater* 1996;8(4):P637.
- [43] Kai W, He Y, Asakawa N, Inoue Y. Effect of lignin particles as a nucleating agent on crystallization of poly(3-hydroxybutyrate). *J Appl Polym Sci* 2004;94(6):2466–74.